Indian Academy of Sciences, Bengaluru
Indian National Science Academy, New Delhi
The National Academy of Sciences India, Prayagraj

SUMMER RESEARCH FELLOWSHIPS — 2024

Format for the final Report *,^

Name of the candidate	:	Md Ashraf
Application Registration no.	:	EPSS201
Date of joining	:	13 May 2024
Date of completion	:	13 July 2024
Total no. of days worked	:	62
Name of the guide	:	Dr. Attreyee Ghosh
Guide's institution	:	Indian Institute of Science, Bangalore
Project title	:	To Estimate The Co-Seismic Surface Deformation Using GPS Measurement

Address with pin code to which the certificate could be sent:

Diamond Hostel IIT (ISM), Dhanbad
Jharkhand- 826004
E-mail ID: 23mc0049@iitism.ac.in
Phone No: 8434587197

TA Form attached with final report : YES ✓ NO _____

If, NO, Please specify reason

Md. Ashraf
Signature of the candidate
Date: 15-07-2024

Signature of the guide
Date: 15/7/2024

IMPORTANT NOTES:

*** This format should be the first page of the report and should be stapled with the main report. The final report could be anywhere between 20 and 25 pages including tables, figures etc.**

^ The final report must reach the Academy office within 10 days of completion. If delayed fellowship amount will not be disbursed.

(For office use only; do not fill/tear)

Candidate's name:	Fellowship amount:
Student: Teacher:	Deduction:
Guide's name:	TA fare:
KVPY Fellow: INSPIRE Fellow:	Amount to be paid:
PFMS Unique Code:	A/c holder's name:
Others	

ACKNOWLEDGEMENT

I express immense gratitude to everyone who supported my project, **"To Estimate the Co-Seismic Surface Deformation Using GPS Measurement"**.

First, I express my deepest gratitude to **Dr. Attreyee Ghosh** at the **Centre for Earth Sciences, Indian Institute of Science (IISc) Bangalore**, for her unwavering support, insightful guidance, and expertise in Geodynamics. Her suggestions, constructive feedback, and encouragement were crucial throughout completing this project report.

I am very thankful to **Dr. Prabhat Kumar** for his continuous support and guidance. His expertise and advice were invaluable in overcoming challenges and advancing my research.

I am grateful to the entire Computational-Geodynamics Lab team for their support and encouragement throughout this project. Their help and collaboration were crucial to its success.

I am grateful to the faculty of Applied Geophysics at IIT (ISM), Dhanbad, for their comprehensive teachings and rigorous curriculum, which enhanced my knowledge and skills.

I also thank the Indian Academy of Sciences for providing me with this invaluable opportunity. Their Summer Research Fellowship Program has been instrumental in allowing me to undertake this project at the Indian Institute of Science (IISc) Bangalore. The exposure and experience gained during this internship have immensely benefited my academic and professional growth.

I am grateful to my friends for their insights, discussions, and assistance, which helped me overcome challenges and stay motivated.

Lastly, my heartfelt gratitude goes to my family for their unconditional love, unwavering support, and belief in my abilities.

To all who contributed to this project's success, your support, guidance, and encouragement have been invaluable. Thank you.

Md Ashraf
M.Sc (Tech) in Applied Geophysics
Indian Institute of Technology (Indian School of Mines), Dhanbad

TO ESTIMATE THE CO-SEISMIC SURFACE DEFORMATION USING GPS MEASUREMENTS

Md Ashraf[1,†] **and Dr. Attreyee Ghosh**[2,†]

[1]*Indian Institue of Technology (ISM), Dhanbad*
[2]*Indian Institute of Science, Bangalore*

This manuscript was compiled on July 15, 2024

Abstract

Contents

TO ESTIMATE THE CO-SEISMIC SURFACE DEFORMATION USING GPS MEASUREMENTS

Md Ashraf[1,†] **and Dr. Attreyee Ghosh**[2,†]

[1]*Indian Institue of Technology (ISM), Dhanbad*
[2]*Indian Institute of Science, Bangalore*

This manuscript was compiled on July 15, 2024

Abstract

This study investigates the co-seismic surface deformation associated with the 2015 Gorkha earthquake in Nepal using GPS measurements from a network of GPS stations in the Nepal region and IGS stations. Our preliminary studies involved understanding the basics of GPS technology and its application in geosciences, which helped us to process and analyze the data effectively. In this study, we processed the GPS data from 26 permanent GNSS stations in Nepal and 12 International GNSS Service (IGS) stations using the GAMIT/GLOBK software. After that, we generate time-series plots and analyze the changes in the Earth's surface, focusing on the GPS station's North, East, and vertical components. The time series plots reveal a sudden jump in the residual values corresponding to the earthquake event, indicating co-seismic deformation. Our results show significant movement and deformation in the affected areas, with varied responses across different stations. We observed maximum displacements of up to 146.66 cm in the north component, 34.10 cm in the east component, and 124.32 cm in the vertical component. We also estimated the velocities of various stations, demonstrating a clear deformation pattern.

Keywords: *GPS DATA, GAMIT/GLOBK, TIME-SERIES PLOT, CRUSTAL-DEFORMATION, EARTHQUAKE, CNX2RNX*

1. Introduction

On April 25, 2015, at 11:56:25 Nepal Standard Time(UTC Time 06:11:25), a powerful 7.8 magnitude earthquake struck Nepal. The epicentre of this earthquake was near the village of Barpak in the Gorkha district, which is about 85 km northwest of Kathmandu. This earthquake, known as the Gorkha earthquake, resulted in the deaths of 8,962 people and injured 21,952 more, making it the worst disaster in Nepal since 1934.

We know that Nepal is situated on the boundary where the Indian and Eurasian plates collide. We can see from the paper of (Ader et al., 2012) [1] in this region that the Indian plate subducts beneath the southern Tibetan plateau along the main Himalayan thrust fault at a rate of 17 to 21 mm per year. The main reason for this earthquake was accumulated stress over a long period.(Feldl and Bilham, 2006).[2]

After the main earthquake, a series of aftershocks hit the region at regular intervals of 15-30 minutes. On April 26, 2015, a significant aftershock of magnitude 6.9 struck at 12:54 NST, with its epicenter located 17 km south of Kodari, Nepal. In the following day, over 38 aftershocks of magnitude 4.5 or greater occurred, including one of magnitude 6.8. As of November 25, 2015, a total of 417 aftershocks of magnitude 4 or greater had been recorded. Unfortunately, these aftershocks triggered landslides that blocked roads, hindered rescue efforts, and resulted in further loss of life and property.

This study estimates the co-seismic surface deformation caused by the 2015 Gorkha earthquake. We analyzed GPS data collected from various Nepal and International GNSS Service (IGS) stations to achieve this. The GPS data was processed using GAMIT software, which is widely used for high-precision GPS data analysis. By generating a time-series plot of these data, we can observe the changes in the Earth's surface and the Velocity of the GPS station's North, East and vertical components.

Our main goal is to carefully process and analyze this data to understand the ground movements caused by the Gorkha earthquake.

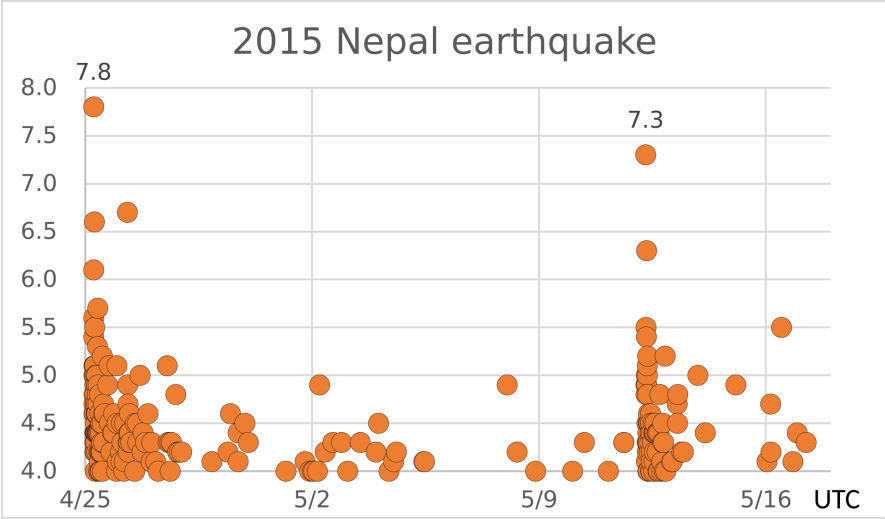

Figure 1. Aftershocks of 2015 earthquake (Source:Wikipedia)

2. Preliminary studies

To understand how earthquakes cause the ground to move, I first needed to learn the basics of GPS technology and how it is used in geosciences. For the basics of GPS, I went through the serc websites (Serc). These resources helped me to understand how GPS works and how it can track the movements of the Earth's surface due to different geological processes. The "Collecting GPS Data" section taught me how GPS technology tracks the movement of the ground, both up and down and side to side. This is important for studying how the ground moves during earthquakes and other natural events.

In the "Earthquake, GPS, and Plate-Motion" section, I learned how GPS could measure ground movement near the edges of tectonic plates, where earthquakes often happen. I studied real-world examples from stations like Saddleback Community College and Belle Mountain in California. The "Glacier, GPS and Sea Level Rise" unit taught me how GPS data can track changes in ground elevation due to melting glaciers. This is useful for understanding long-term changes in glacier mass and their impact on sea levels.

The primary objective of the preliminary studies was to review and understand the methodologies for analyzing GPS data in the context of coseismic deformation.

3. Study Area

In this paper, our study area is situated in the Gorkha region of Nepal, which is approximately located at 28.3°N latitude and 84.72°E longitude. This area was heavily affected by the earthquake.

In this paper, our aim is to understand and analyze the movement of the ground during the Gorkha earthquake (2015) by processing the GPS data from regional sites and IGS stations to understand the earthquake's impact.

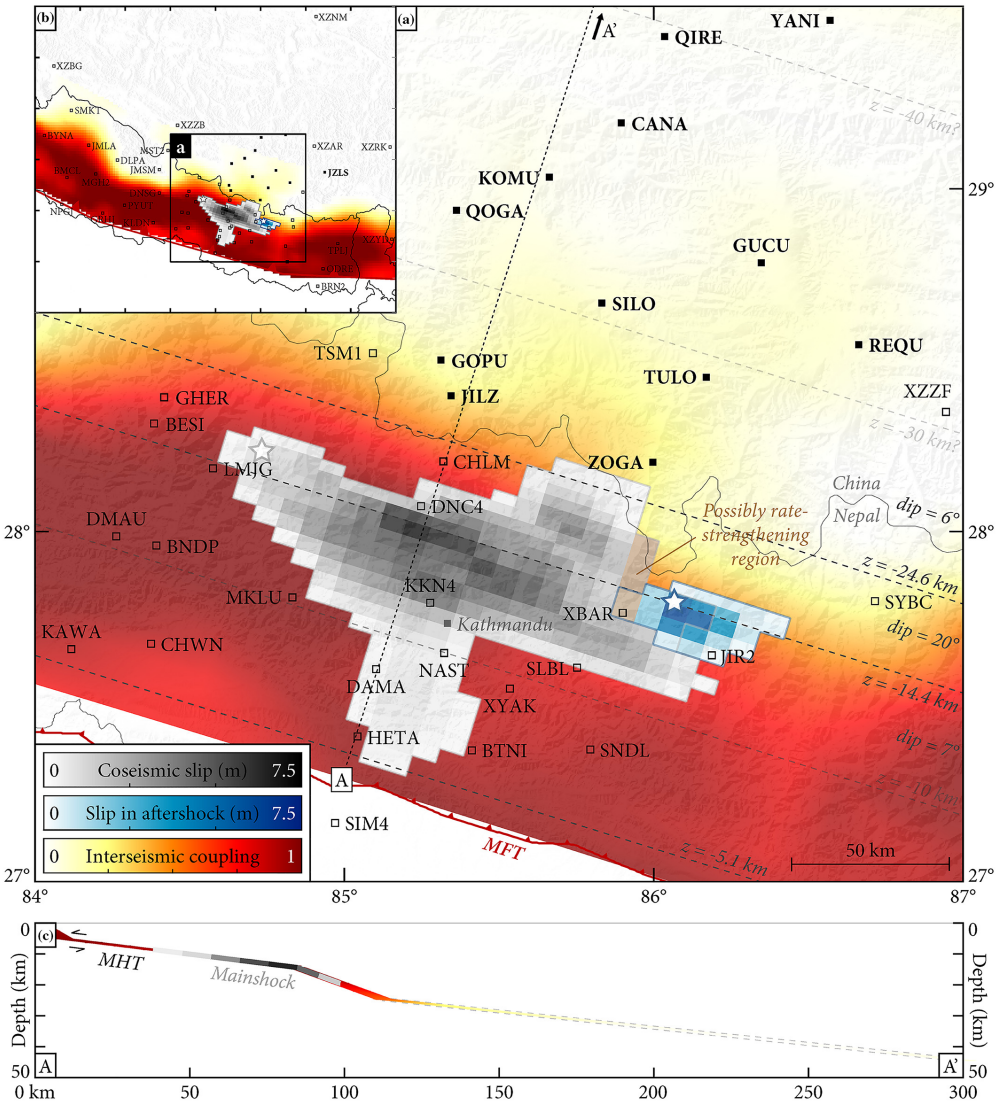

Figure 2. Distribution of GPS stations in the Gorkha region, Nepal: The hollow square stations are GPS stations established in Nepal, and solid square notations stations are outside Nepal. The stations in the white area are in the Gorkha regions.

4. Introduction to GPS

GPS, or the Global Positioning System, is developed and operated by the U.S. Department of Defense and provides synchronization of location, Velocity, and time. GPS allows users to determine their precise location, Velocity, and time.

For positions, the GPS satellite transmits two types of signals:
The L1 signal: These signal types operate at a carrier frequency of 1,575.42 MHz. This signal is the most commonly used. It is used for civilian GPS use and has an accuracy of 1-2 meters. This essential components carried by these signals are-

- **C/A-code(Coarse/Acquisition-code)**: The one millisecond-long pseudorandom noise code, as its chipping rate is around 1 MHz. This code is applied in pseudo-ranges determination for positioning. This is used for civilian use and has lower accuracy than the P-code.
- **P-code (Precision- code)**: A weeklong segment with a chipping rate of about 10 MHz. It provides more precise measurements but is encrypted for military use.

The L2 signal has a carrier frequency of 1,227.60 MHz and is modulated with the P-code and navigation message. Unlike the L1 signal, the L2 signal does not contain the C/A code. This signal is primarily used for military applications and provides accurate location information with an accuracy of 0.5 meters

LC or L3 observations: It is a linear combination of both L_1 and L_2 GPS signals. It is also called the ionosphere-free phase combination. This combination helps us make GPS measurements more accurate by removing most ionospheric delay, which is one of the main sources of error in GPS data.

LC is expressed as

$$L_C = \frac{1}{f_1 + f_2}(f_1 L_1 - f_2 L_2) \tag{1}$$

Where, L_1 and L_2 are the phase measurements and f_1 and f_2 are the frequencies of L_1 and L_2, respectively.

Understanding these types of signals is very important to effectively use GPS technology in various fields, such as navigation, precise positioning, and scientific research.

4.1. How does GPS work?

The GPS relies on a network of 24 satellites orbiting the Earth at an altitude of 20,000 km, moving at a speed of 14,000 km/h. These satellites transmit signals that a GPS device can use to calculate its location, Velocity and elevation using a technique called **trilateration.**

Although a minimum of three satellites are required to determine a location on the Earth's surface, a fourth satellite is often utilized to provide additional validation and accuracy to the data received from the initial three. The inclusion of the fourth satellite also enables the

calculation of altitude.

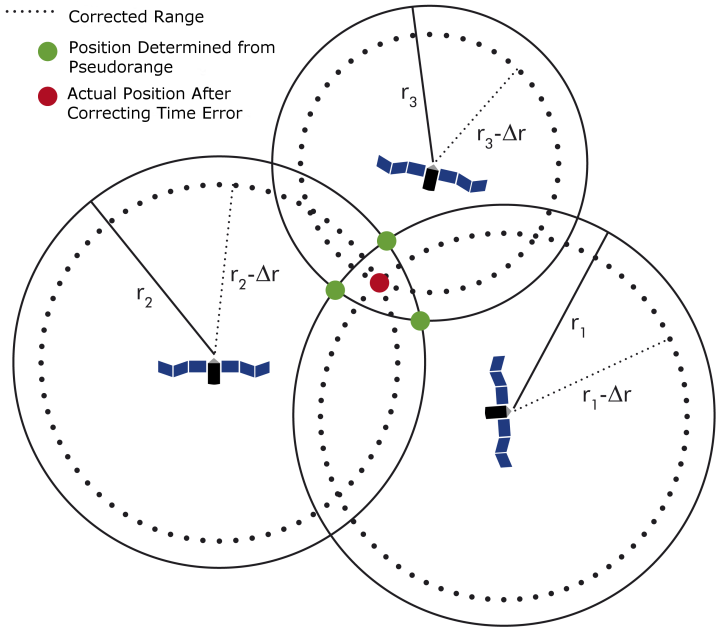

Figure 3. Working of the GPS System

Satellites continuously send signals that GPS devices on or near the Earth's surface receive and interpret. A GPS device needs signals from at least four satellites to accurately determine its location.

Each satellite orbits the Earth twice daily, transmitting a unique signal with orbital details and precise time information. This allows a GPS device simultaneously to receive signals from multiple satellites, typically six or more at any given time.

Each GPS satellite has four atomic clocks to be sure that one is always working. Each clock cost is around 100000 USD and accurate to 1 billionth of the seconds($10^{-9}s$)

When a satellite sends out a signal, it creates a sphere around itself with the GPS device on its surface. By receiving signals from multiple satellites, the GPS device can calculate its distance from each satellite, forming spheres around each one.

Adding more satellites means more intersecting spheres. With signals from three satellites, the location of the GPS device can be pinpointed where these spheres intersect. In a three-dimensional space, these intersections typically yield two possible points. The point nearest to Earth is selected as the device's location.

4.2. Sources of GPS Error

In GPS, an error is the difference between the measured or calculated position and the true position of a GPS receiver or an object being tracked.
Some GPS error sources(Karaim, Malek, et al. 2017)[3] are given as-

1. **Selective Availability :** Historically, the U.S. Department of Defense introduced intentional errors in the GPS signals for national security reasons, a practice known as Selective Availability (SA). Although SA has been turned off since 2000, it was a significant source of error in earlier GPS measurements.
2. **Satellite orbit irregularities:** The orbital path of GPS satellites can deviate slightly from their predicted paths due to gravitational influences and other factors. These deviations can cause positional inaccuracies.
3. **Satellite and Receiver-clock errors:** As we know, GPS satellites have highly accurate atomic clocks. This means that even tiny inaccuracies in the satellite clock can lead to errors in the satellite's time signals, which can lead to mistakes in determining the user's location
4. **Atmospheric delay:** Atmospheric-delay condition refers to the effects of the Earth's atmosphere on GPS signals as they pass through it. The atmosphere can cause delays in the signals, which can lead to errors in GPS positioning.
   There are two main types of atmospheric delay:
   (a) **Ionospheric delay:** The ionosphere, a layer of the atmosphere extending from about 48 to 965 km altitude, can slow down GPS signals due to the presence of free electrons. This delay is frequency-dependent and can be significant, especially during periods of high solar activity
   (b) **Tropospheric-delay:** Troposphere is the lowest layer of the atmosphere. The presence of water vapour and other gases in this layer can slow down GPS signals. This delay is related to atmospheric pressure, temperature, and humidity.
5. **Multipath:** GPS signals can bounce off surfaces like buildings, trees, and the ground before reaching the receiver. These reflected, or multipath signals interfere with the direct signals, leading to positional errors.
6. **Ephemeris Data Errors:** The information about the satellite's position in its orbit (ephemeris data) can contain errors. These errors propagate into the calculated position of the GPS receiver.
7. **Human Errors:** Errors can also be caused by human factors, such as errors in the installation, operation, and interpretation of GPS equipment data. Proper training and rigorous procedures are essential to minimize these errors.

4.3. How Can Studying GPS Motion Be Useful To Society?

GPS technology is a powerful tool for monitoring natural and anthropogenic phenomena.GPS technology can measure a wide range of phenomena, including:

1. Movement of ground
    - Due to plate motion.
    - Near earthquake faults.
    - During earthquakes.
    - Due to the changing size of glaciers.
    - Due to the movement of magma underground
    - Due to changing snow depth
    - Due to changing amount of groundwater.
    - Due to the changing size of the lakes and reservoirs
    - From a landslide
2. Amount of water in the atmosphere
3. Amount of soil moisture
4. Vegetation growth
5. Sea level
6. Amount of ash in the atmosphere

5. METHODOLOGY

5.1. Fundamental of GAMIT/GLOBK

GAMIT (GNSS at MIT) is widely used in the field of GPS data processing and Geodesy. The software was developed by MIT, Scripps Institution of Oceanography, and Harvard University with the support of the National Science Foundation. It is a collection of programs to process phase data to estimate three-dimensional relative positions of ground stations and satellite orbits, atmospheric zenith delays, and Earth orientation parameters. The software is designed to run on any UNIX operating system.[2]

GLOBK ("Global Kalman filter") is a Kalman filter whose primary purpose is to combine various geodetic solutions such as GPS, VLBI, and SLR experiments. It accepts as data, or "quasi-observations", the estimates and covariance mamatricesor station coordinates, Earth orientation parameters, orbital parameters, and source positions generated from the analysis of the primary observations. The input solutions are generally performed with loose a priori uncertainties assigned to all global parameters so that constraints can be uniformly applied in the combined solution.

5.2. Application of GAMIT/GLOBK in earth science

GAMIT/GLOBK is a powerful software tool used to process GNSS data with high precision, having numerous applications in the field of earth sciences. It plays a pivotal role in monitoring plate-tectonic motion and regional crustal movement. By analyzing data from GPS stations worldwide, GAMIT/GLOBK helps us to understand how Earth's tectonic plates shift and interact over time. (Avouac and Tapponnier, 1993; Altamimi et al., 2012, 2016; Wang, 2020)[4]; Zhang et al., 2005; Bettinelli et al., 2006; Bilham et al., 1997) [5]

GAMIT/GLOBK is frequently integrated with seismic fault distributions to investigate the entire seismic process, from earthquake preparation and occurrence to the subsequent healing of crustal deformation. The intermediate data generated by GAMIT/GLOBK, such as tropospheric delay measurements, are valuable for studying atmospheric water vapour content and enhancing weather forecasting. Additionally, it measures the total ionospheric electron content, which can be used to monitor cosmic particle activities and predict electromagnetic events such as geomagnetic storms (Ciraolo et al., 2007; Zakharenkova et al., 2008)[6] It is used to monitor earthquake and volcanic activity, enabling scientists to better understand these natural phenomena. The software's ability to analyze atmospheric water vapour content also enhances weather forecasting.

5.3. Downloading the GPS Data

For the installation of the GPS data, I explored several websites such as UNAVCO, SOPAC, and CDDIS. Additionally, I utilized the GAMIT/GLOBK software to obtain the RINEX (Receiver Independent Exchange) data for several GPS stations in Nepal (BESI, DMAU, KKN4, KIRT, NAST, SNDL, CHLM, SIM4, HETA, SLBL, LMJG, CHWN, GHER, SYBC, RMJT, MKLU, JIR2, XYAK, BNDP) and IGS stations (HYDE, IISC, LCK4, TASH, POL2, BJFS, HKSL, HRAO, BAKO,

CUSV, BADG, BHR4, ARTU, TWTF, HARB, DRAG).

For this purpose, I set up the GAMIT/GLOBK software. GAMIT is a collection of programs that are used to analyze and process GPS data.

For the data downloaded from the UNAVCO website (GNSS Data Access 3.0) which is in the CNX(Coordinate Network Exchange) format, it is necessary to convert the CNX format data to RNX format this, I used CNX2RNX, a tool developed by Y. Hatanaka.

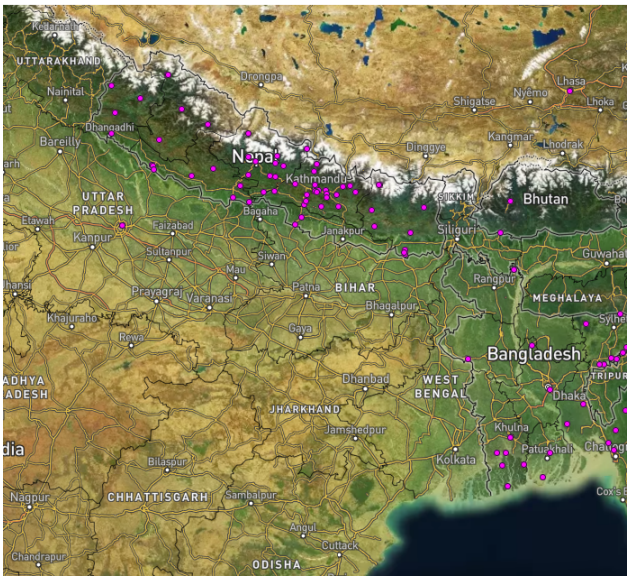

Figure 4. GNSS Permanent Station Data sites: The Magenta circle is the GPS stations

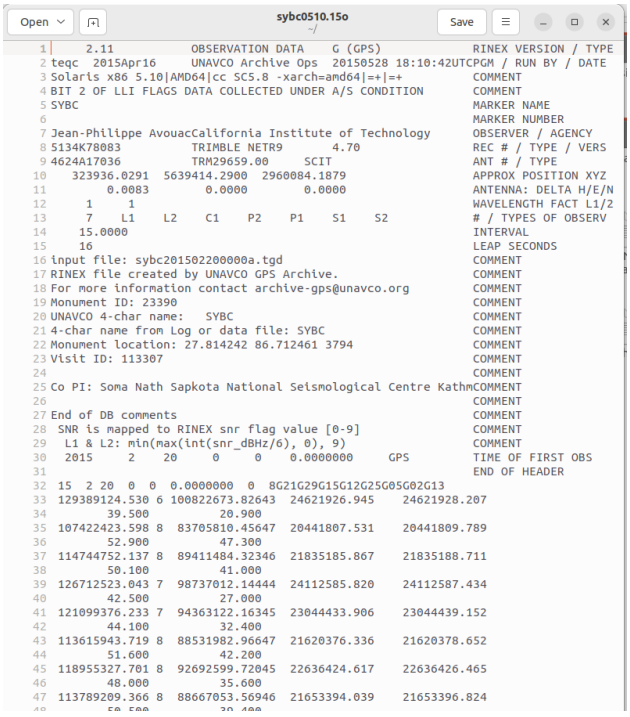

Figure 5. Rinex data format for the SYBC station

5.4. Continuous GPS Measurements in Gorkha Region, Nepal

We obtained continuous daily observation data (Kumar, Prabhat et al.)[7] for up to 5 years from the 26 new permanent GNSS stations. However, We processed the GPS data only for ten days in February and ten days in August, at six-month intervals, from 2010 to 2016 across all stations by using GAMIT v10.7 (T. A. Herring et al. 2003) [8] alongside the data from 12 IGS stations (ARTU, IISC, HYDE, BJFS, TASH, BAKO, BADG, CUSV, COCO, POL2, DRAG, HARB, TWTF) in baseline mode to derive loosely constrained site coordinates in the ITRF 2014 reference frame (Altamimi et al., 2016; Rebischung et al., 2016) [9]. The IGS stations included in our solutions were selected based on their data availability and their geographic distribution around our network.

We used the FES2004 model, combined IGS Total Electron Content Maps (Feltens Schaer, 1998)[10] and Vienna Mapping Functions (VMF1) (Boehm Schuh, 2003; J. Kouba, 2008)[11] to remove the ocean tidal loading, ionospheric, and tropospheric effects, respectively, from the phase solution. The IERS2010 model was used to correct for the perturbations caused by solid earth tides.

6. GPS Data Processing

In this study, we used the GAMIT/GLOBK software to process our GPS data obtained from the different stations, and obtain daily, loosely constrained solutions, and positions for each GPS station. The processing was carried out using a double-difference method that relied on precise satellite orbits and clocks from the International GNSS Service (IGS), Earth rotation parameters (ERPs), and global ionosphere models. For the estimation of the hydrostatic and wet zenith delays(WZD) for the troposphere model, I used the Vienna Mapping Function(VMF1). We used the FES2004 model for ocean tide loading, which is referenced to the Centre of Mass (CM) frame. We combined regional and global solutions to create daily solutions that included coordinates and their corresponding covariance.

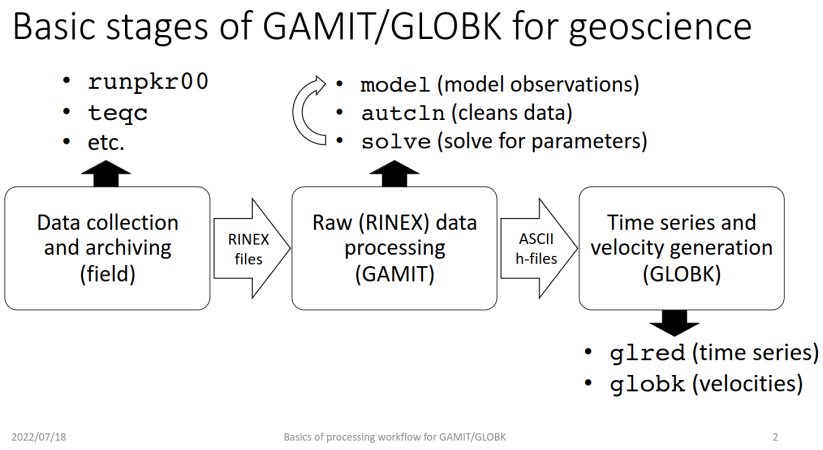

Figure 6. Processing workflow (M. A. Floyd, T. A. Herring)

6.1. Multipath and Water Vapor Effects in the Observations:

Multipath occurs when GPS signals reflect off surfaces before reaching the receiver, causing interference with the direct signal.[5]
To reduce this effect:

1. **Avoid Reflective Surfaces:** Place GPS receivers away from surfaces that can reflect signals.
2. **Use a Ground Plane Antenna:** This helps to minimize signal reflections.
3. **Avoid Near-Ground Mounts:** Mount antennas at a higher position to reduce ground reflections.
4. **Observe for Many Hours:** Longer observation periods can help avoid multipath errors.
5. **Average Data from Multiple Days:** Combining data over several days helps mitigate multipath effects' impacts.

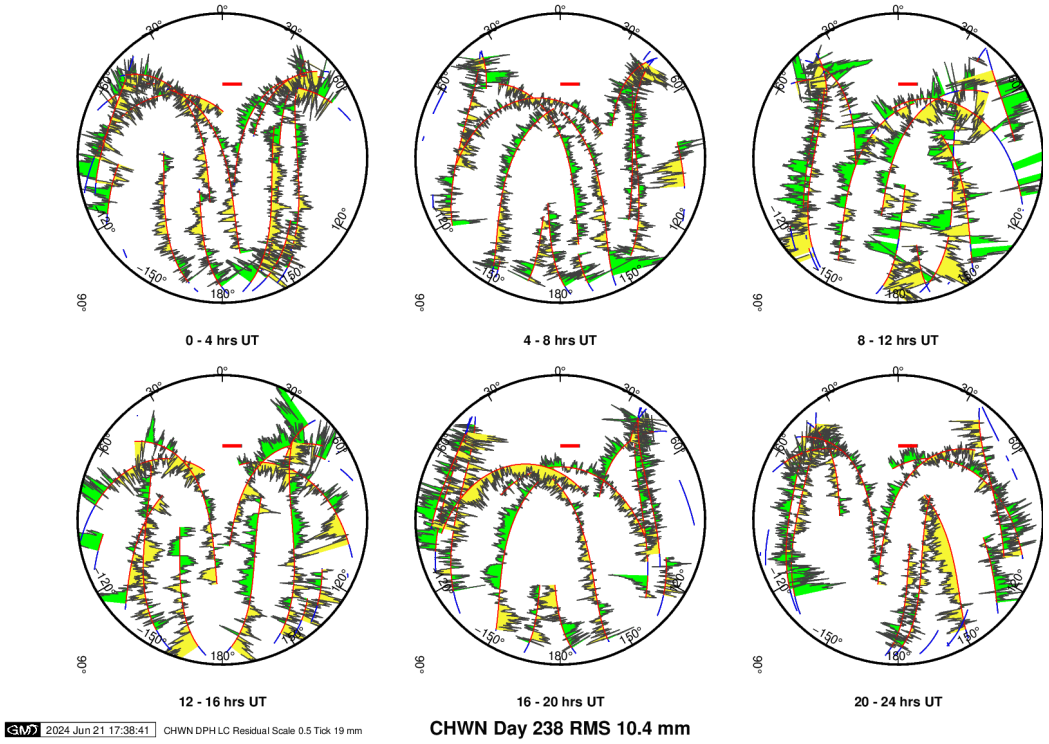

Figure 7. SKY-plot

In our analysis, we projected one-way (undifferenced) LC phase residuals onto the sky in 4-hour snapshots. Spatially repeatable noise was identified as multipath, while time-varying noise was attributed to water vapour. In these projections, **the satellite track is depicted in red**. For visual effect, **positive residuals are shown in yellow** and **negative residuals in green**. A **red bar** was included for reference.

High residuals in the same place at different times suggest multipath (0-4, 4-8 and 8-12 hours). High residuals appearing in a given place only at one time suggest water vapour.

Normal pattern: These types of bands are high-frequency multipath; red is the smoothing of individual values, showing no strong systematics. Mid-elevation angle noise could be atmospheric delay errors.

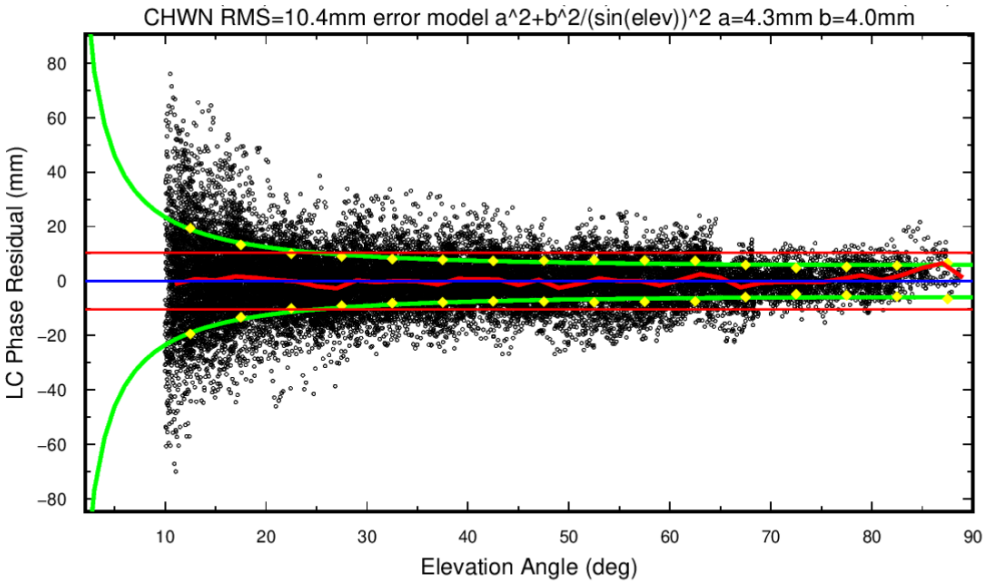

Figure 8. Phase-Residual vs Elevation angle

This figure(8) illustrates the relationship between the LC (L3) phase residuals and the elevation angle for the GNSS station CHWN.

The plot shows a larger spread of residuals at lower elevation angles, which decreases as the elevation angle increases. This trend is typical in GNSS measurements due to increased errors such as multipath and atmospheric delays at lower angles. The green lines closely follow the scatter of the residuals, suggesting that the error model accurately captures the behaviour of the residuals. The RMS value of 10.4 mm provides a measure of the average residual error, indicating the overall accuracy of the phase measurements for this station.

7. Results

7.1. Time series plot

A time series is a graph that shows how positions change over time, typically showing the changes in the coordinate residuals(North, East and Up) at a specific station or location.

In the context of GPS data, a time series plot can reveal various features, such as:

1. **Coseismic deformation:** A sudden jump or change in the residual values corresponding to an earthquake event, indicating the ground deformation caused by the earthquake.
2. **Post-seismic deformation:** A gradual change in the residual values after an earthquake indicates the Earth's surface deformation.
3. **Seasonal and annual signals:** Periodic variations in the residual values due to atmospheric and oceanic loading, thermal expansion, and other environmental factors.
4. **Instrumental and data quality issues:** Anomalies or outliers in the data may indicate problems with the GPS instrument, data transmission, or processing.

By analyzing GPS time series plots, researchers and geodesy experts can:

(a) Estimate coseismic deformation and study earthquake mechanics.
(b) Monitor post-seismic deformation and understand the viscoelastic response of the Earth's crust.
(c) Remove seasonal and annual signals to isolate the secular deformation signal.
(d) Identify and correct instrumental and data quality issues.

In this section, we present the time-series plots of the GPS data after processing, which shows the variations in coordinates residual over time. These plots are essential in identifying the coseismic deformation during the earthquake and the Velocity of the GPS stations and estimating the magnitude and its directions.

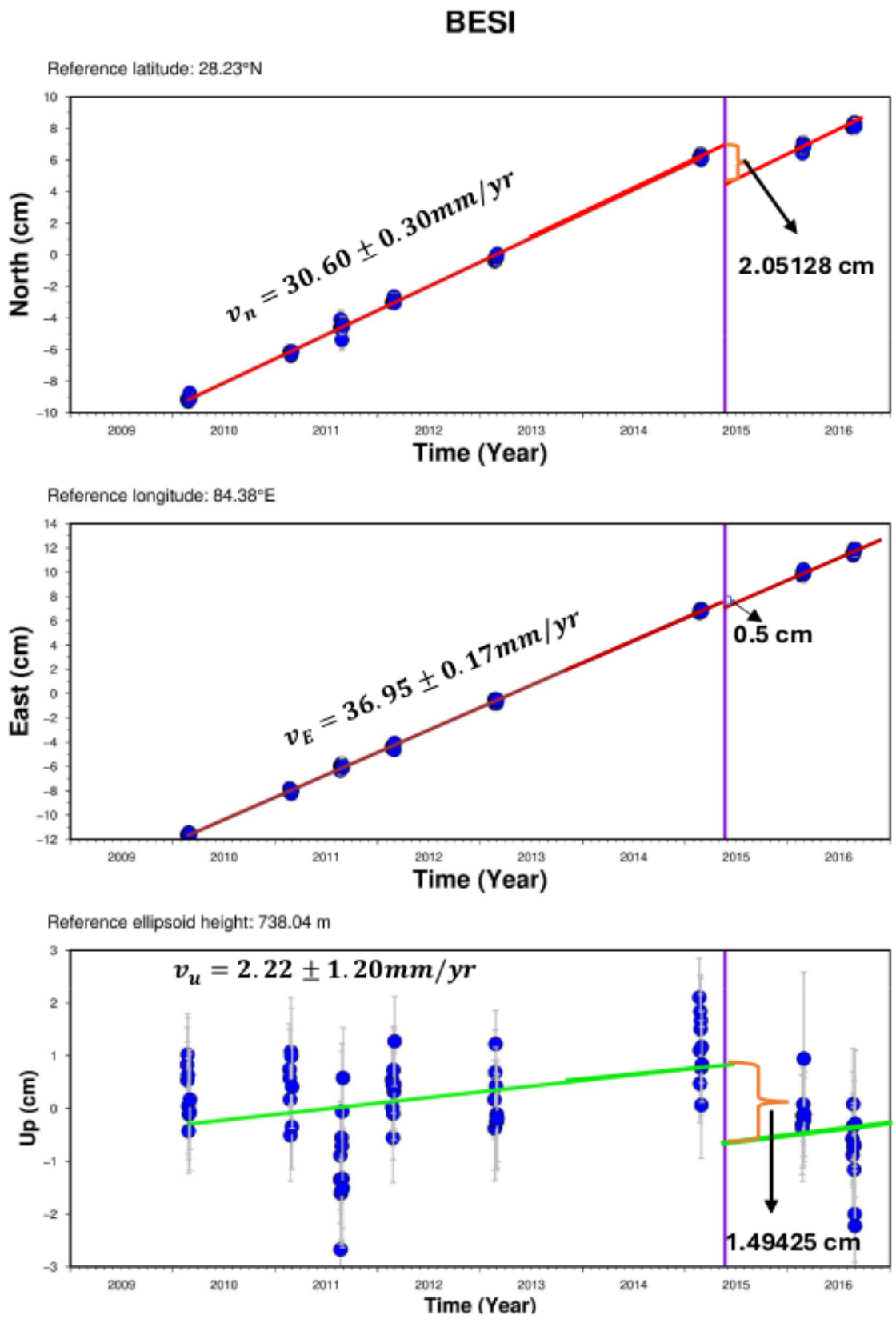

Figure 9. The Velocity of the North component of the station BESI is 30.60±0.30 mm/yr, the East component is 36.95±0.17 mm/yr, and the vertical component is 2.22±1.20 mm/yr. The crustal deformation of the surface is 2.05128 cm, 0.5 cm, and 1.49425 cm, corresponding to the North, East, and Vertical directions, respectively.

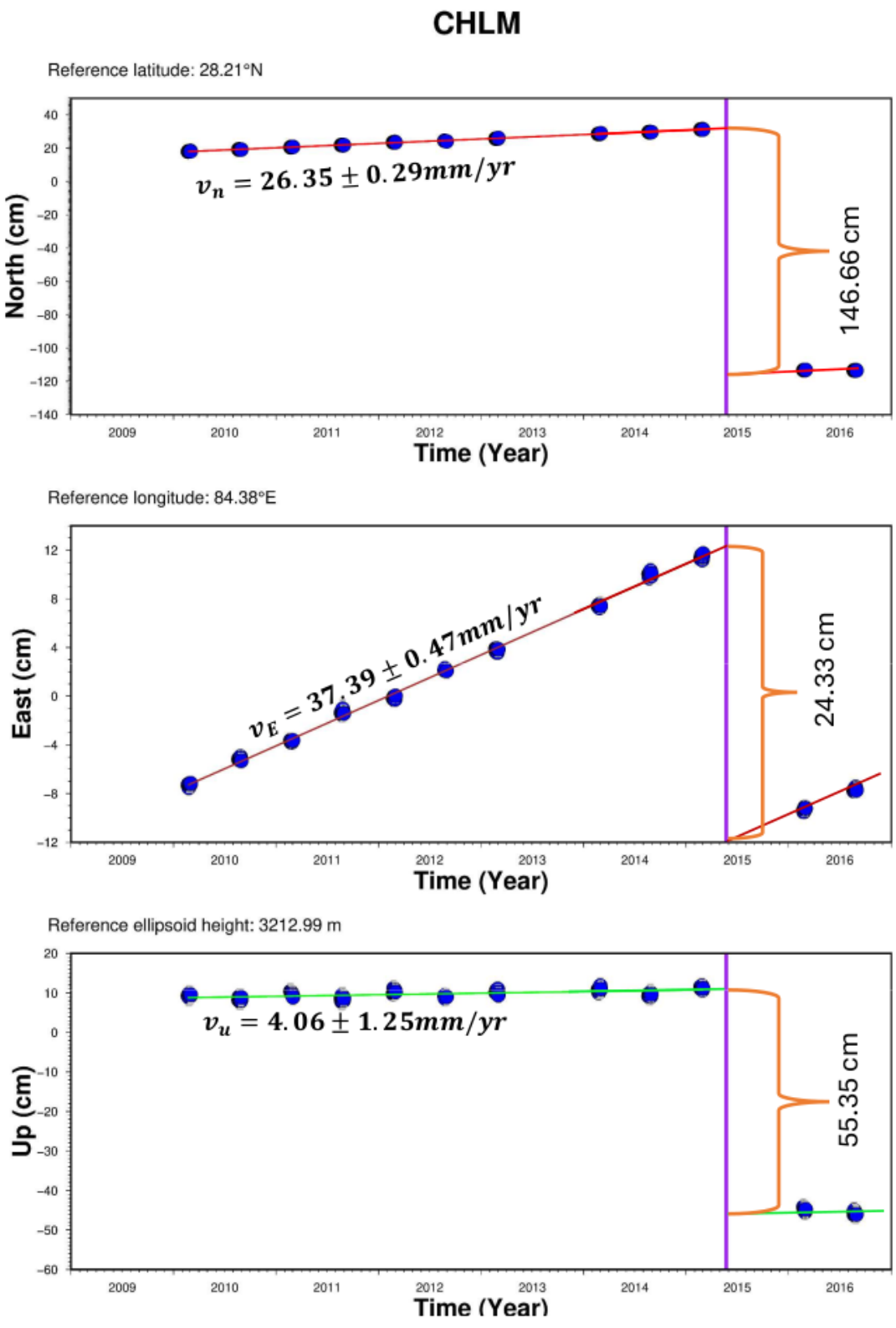

Figure 10. The Velocity of the North component of the station chlm is 26.35±0.29 mm/yr, the East component is 37.39±0.47 mm/yr, and the vertical component is 4.06±1.25 mm/yr. The crustal deformation of the surface is 146.66 cm, 24.33 cm, and 55.35 cm, corresponding to the North, East, and Vertical directions, respectively.

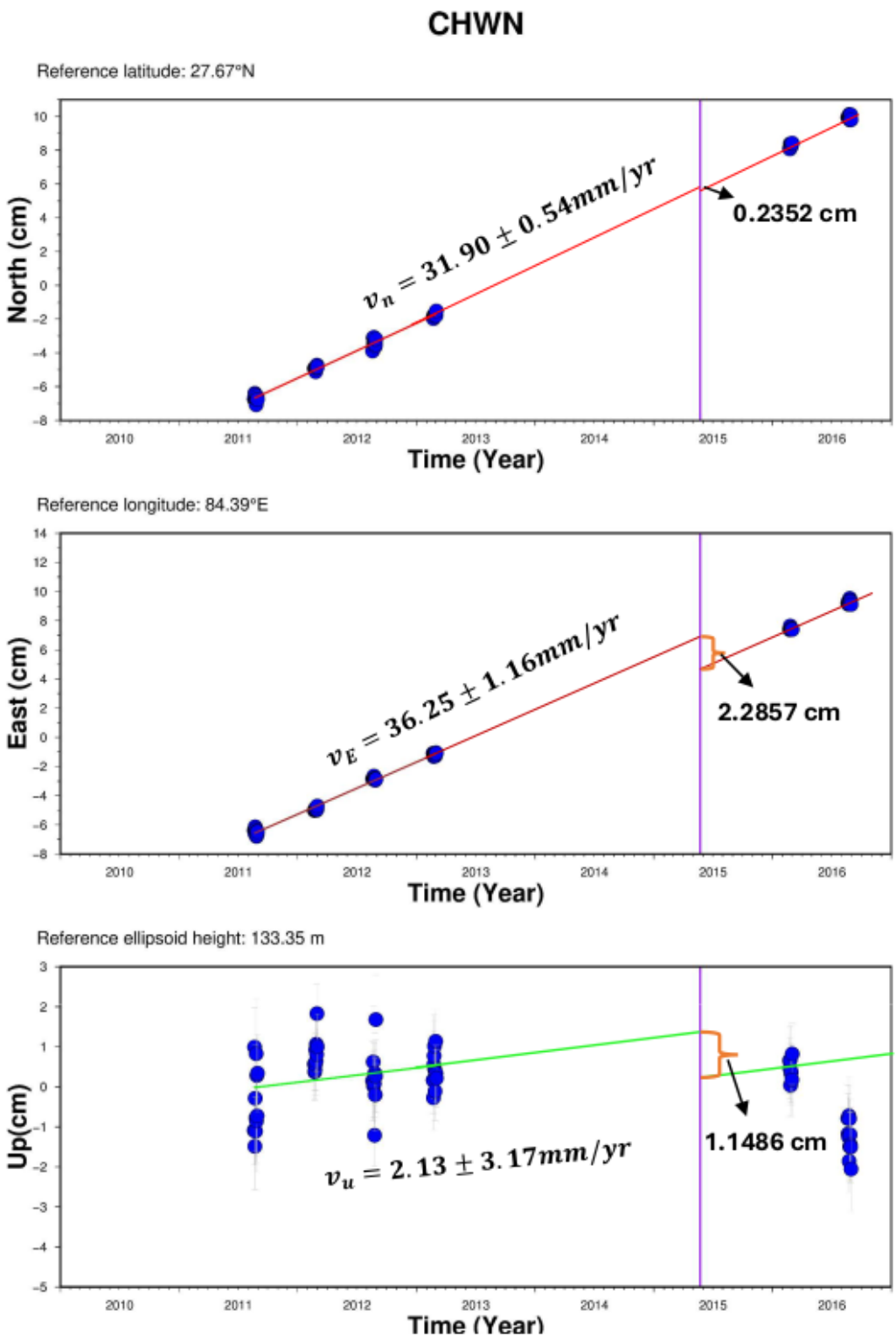

Figure 11. The Velocity of the North component of the station CHWN is 31.90±0.54 mm/yr, the East component is 36.25±1.16 mm/yr, and the vertical component is 2.13±3.17 mm/yr. The crustal deformation of the surface is 0.2352 cm, 2.2857 cm, and 1.1486 cm, respectivel,, corresponding to the North, East, and Vertical directions.

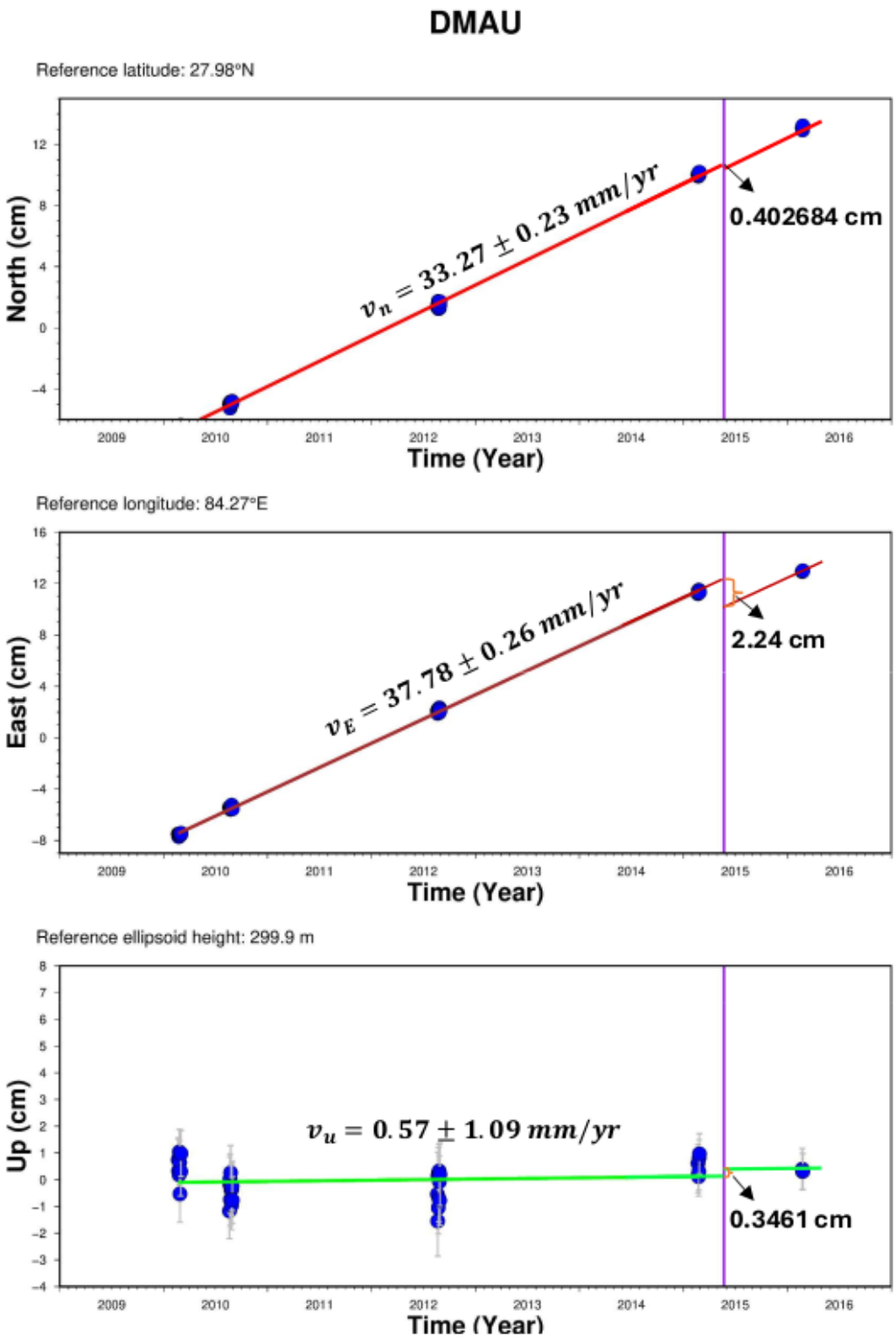

Figure 12. The Velocity of the North component of the station DMAU is 33.27±37.78 mm26r, the East component is 37.78±0.26 mm/yr, and the vertical component is 0.57±1.09 mm/yr. The crustal deformation of the surface is 0.402684 cm, 2.24 cm, and 0.3461 cm, respectively,, corresponding to the North, East, and Vertical directions.

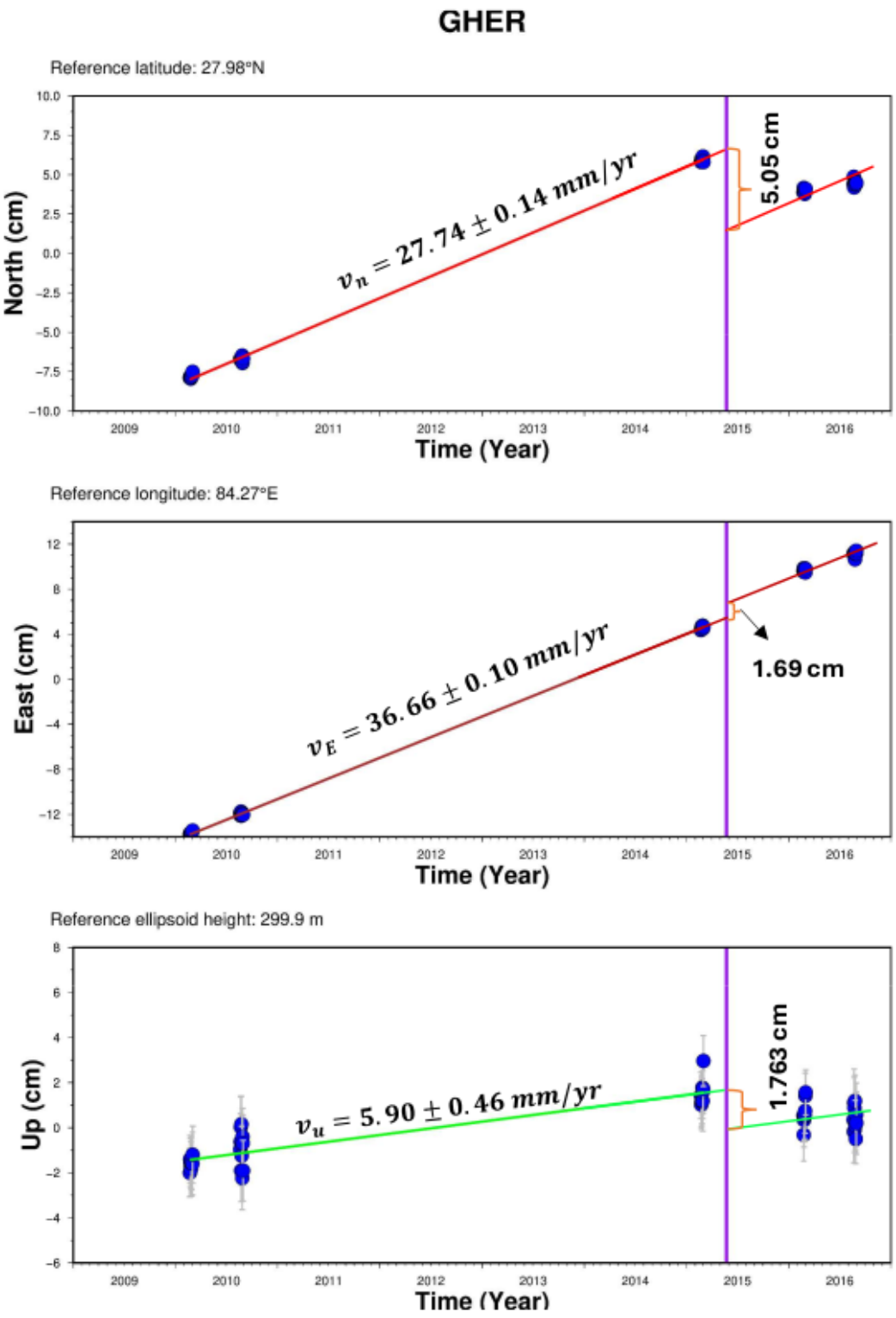

Figure 13. The Velocity of the North component of the station GHER is 27.74±0.14 mm/yr, the East component is 36.66±0.10 mm/yr, and the vertical component is 5.90±0.46 mm/yr. The crustal deformation of the surface is 5.05 cm, 1.69 cm, and 1.763 cm, corresponding to the North, East, and Vertical directions, respectively.

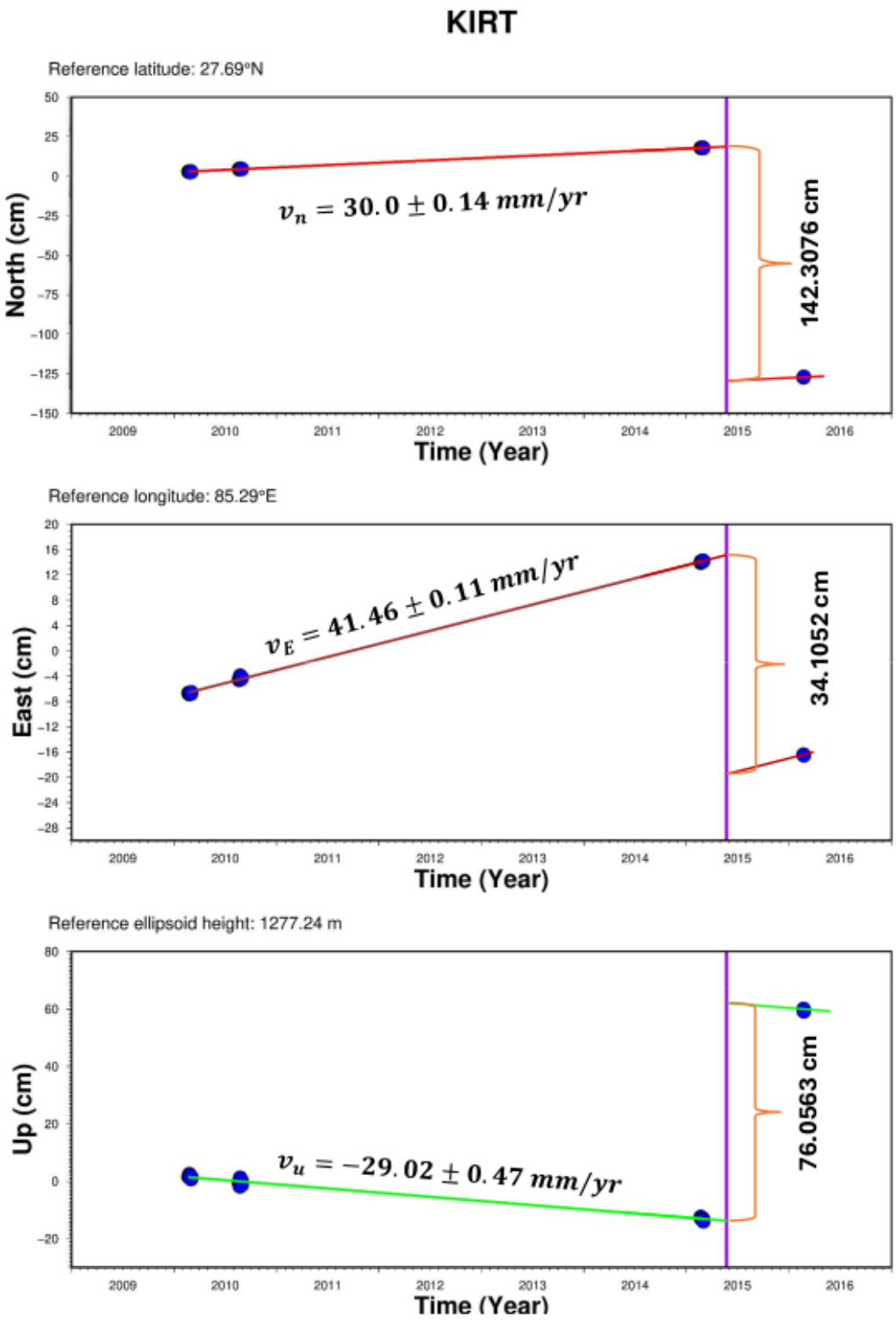

Figure 14. The Velocity of the North component of the station KIRT is 30.0±0.14 mm/yr, the East component is 41.46±0.11 mm/yr, and the vertical component is -29.02±0.47 mm/yr. The crustal deformation of the surface is 142.3076 cm, 34.1052 cm, and 76.0563 cm, corresponding to the North, East, and Vertical directions, respectively.

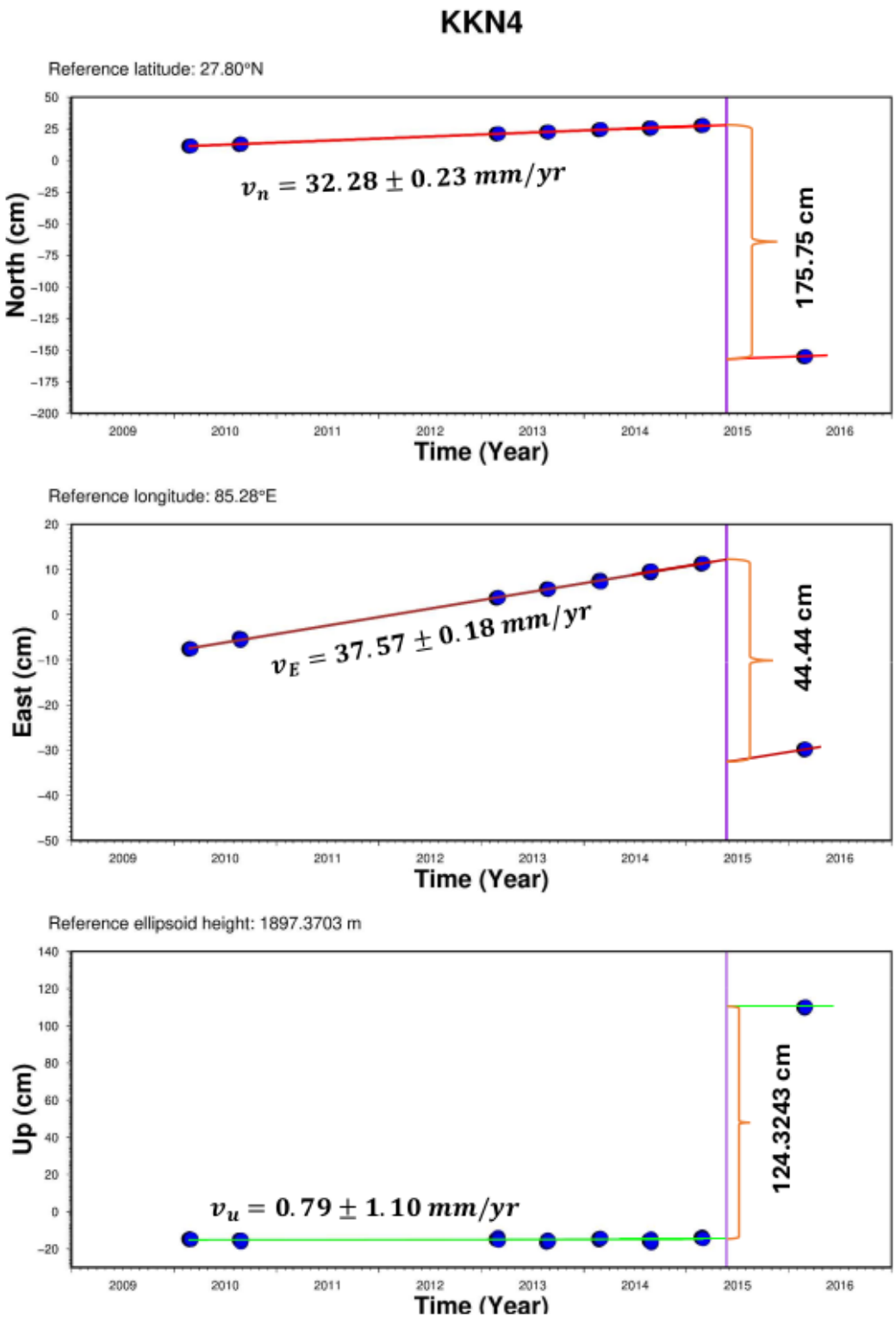

Figure 15. The velocity of the North component of the station KKN4 is 32.28±0.23 mm/yr, the East component is 37.57±0.18 mm/yr, and the vertical component is 0.79±1.10 mm/yr. The crustal deformation of the surface is 175.75 cm, 44.44 cm, and 124.3243 cm, corresponding to the North, East, and Vertical directions, respectively.

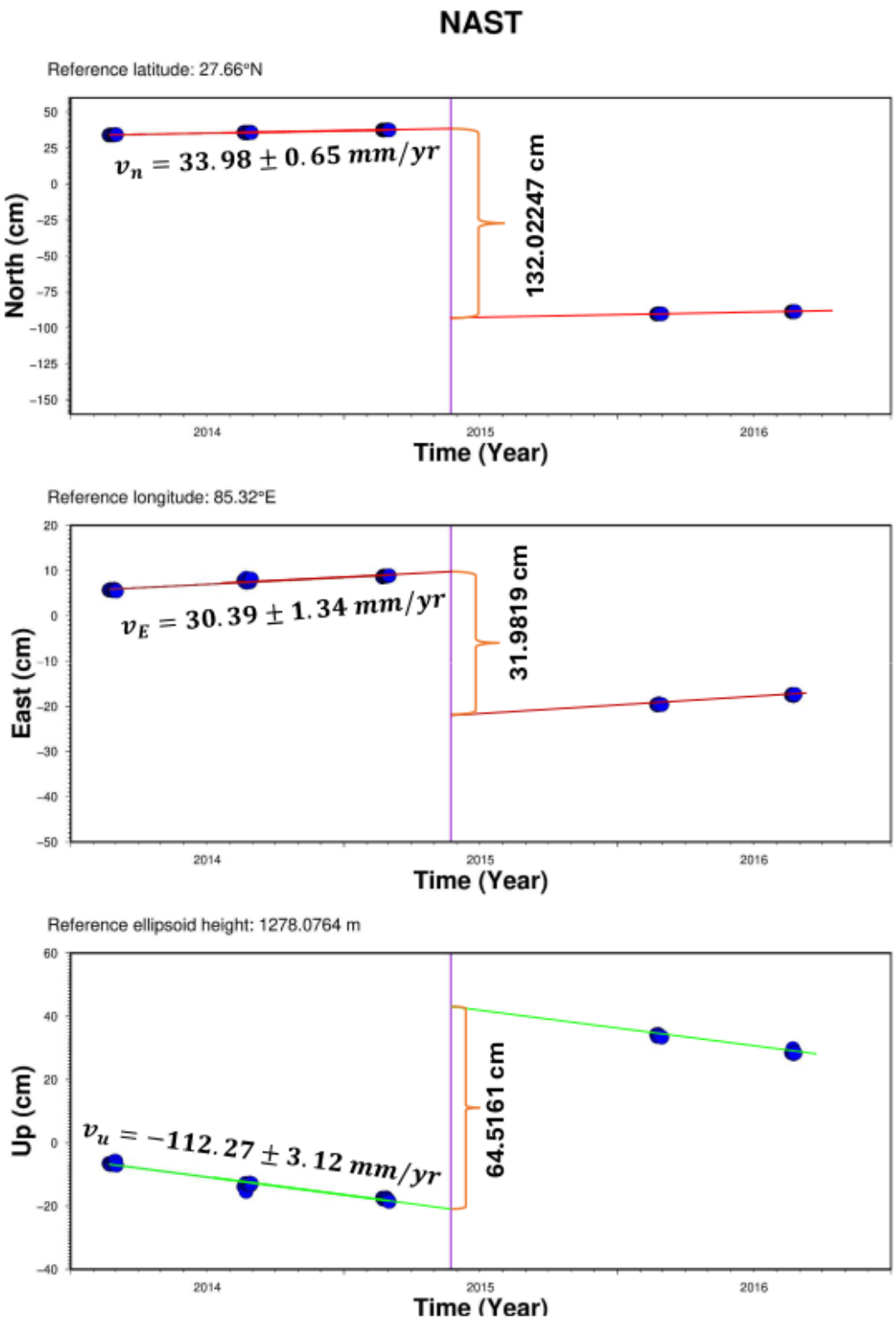

Figure 16. The Velocity of the North component of the station NAST is 33.98±0.65 mm/yr, the East component is 30.39±1.34 mm/yr, and the vertical component is -112.27±3.12 mm/yr. The crustal deformation of the surface is 132.02247 cm, 31.9819 cm, and 64.5161 cm, corresponding to the North, East, and Vertical directions, respectively.

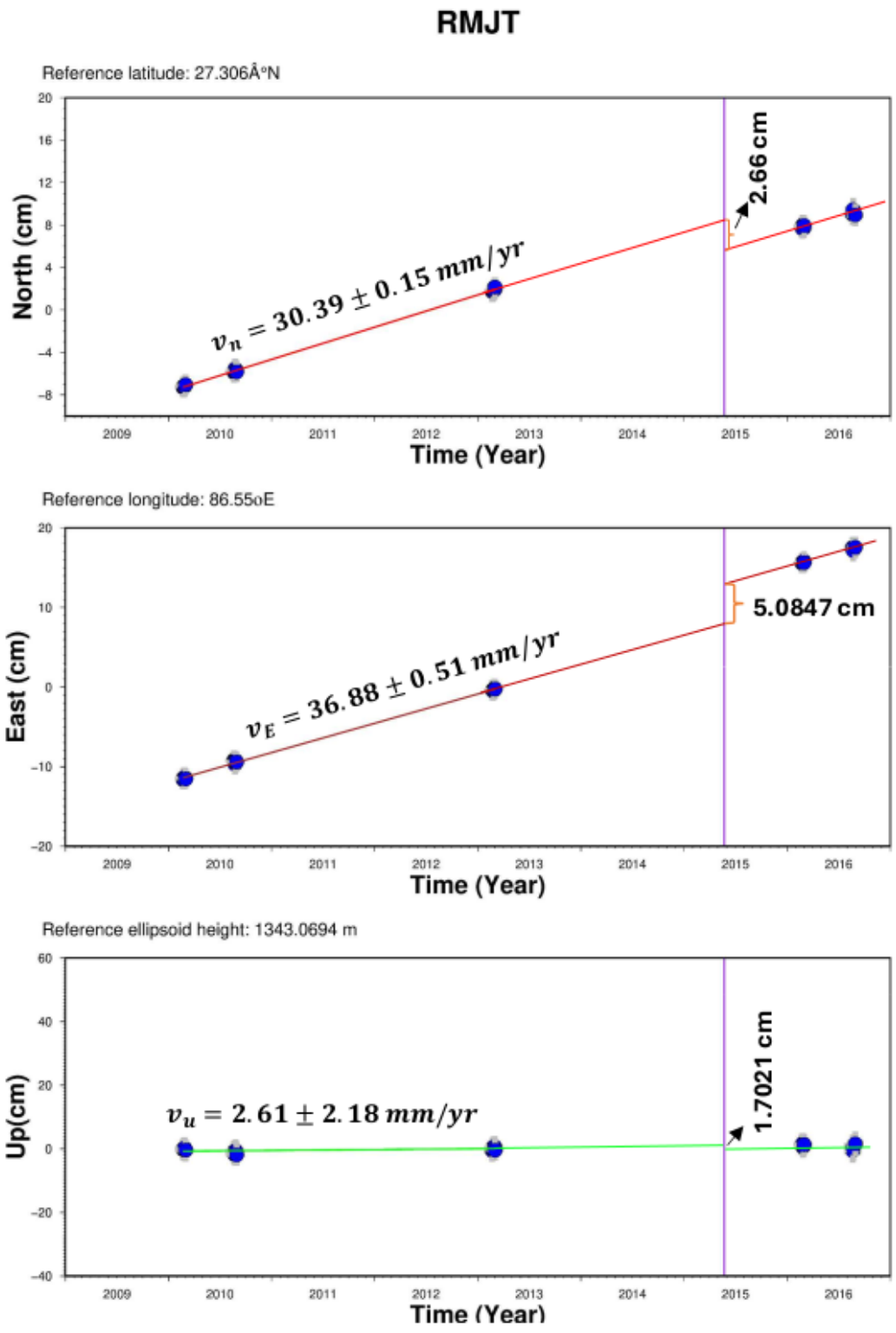

Figure 17. The Velocity of the North component of the station RMJT is 30.39±0.15 mm/yr, the East component is 36.88±0.51 mm/yr, and the vertical component is 2.61±2.18 mm/yr. The crustal deformation of the surface is 2.66 cm, 5.0847 cm, and 1.7021 cm, corresponding to the North, East, and Vertical directions, respectively.

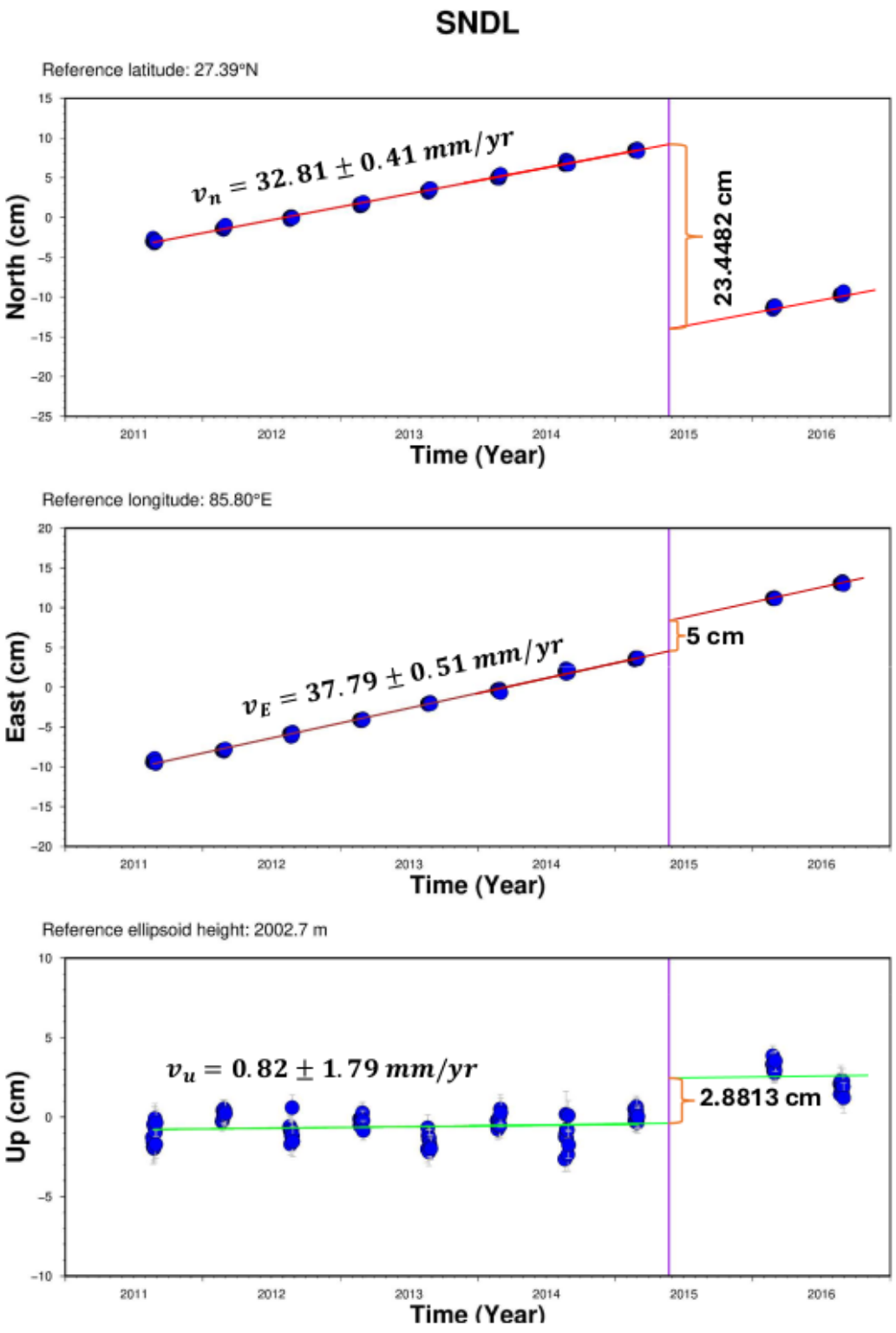

Figure 18. The Velocity of the North component of the station SNDL is 32.81±0.41 mm/yr, the East component is 37.79±0.51 mm/yr, and the vertical component is 0.82±1.79 mm/yr. The crustal deformation of the surface is 23.4482 cm, 5 cm, and 2.8813 cm, corresponding to the North, East, and Vertical directions, respectively.

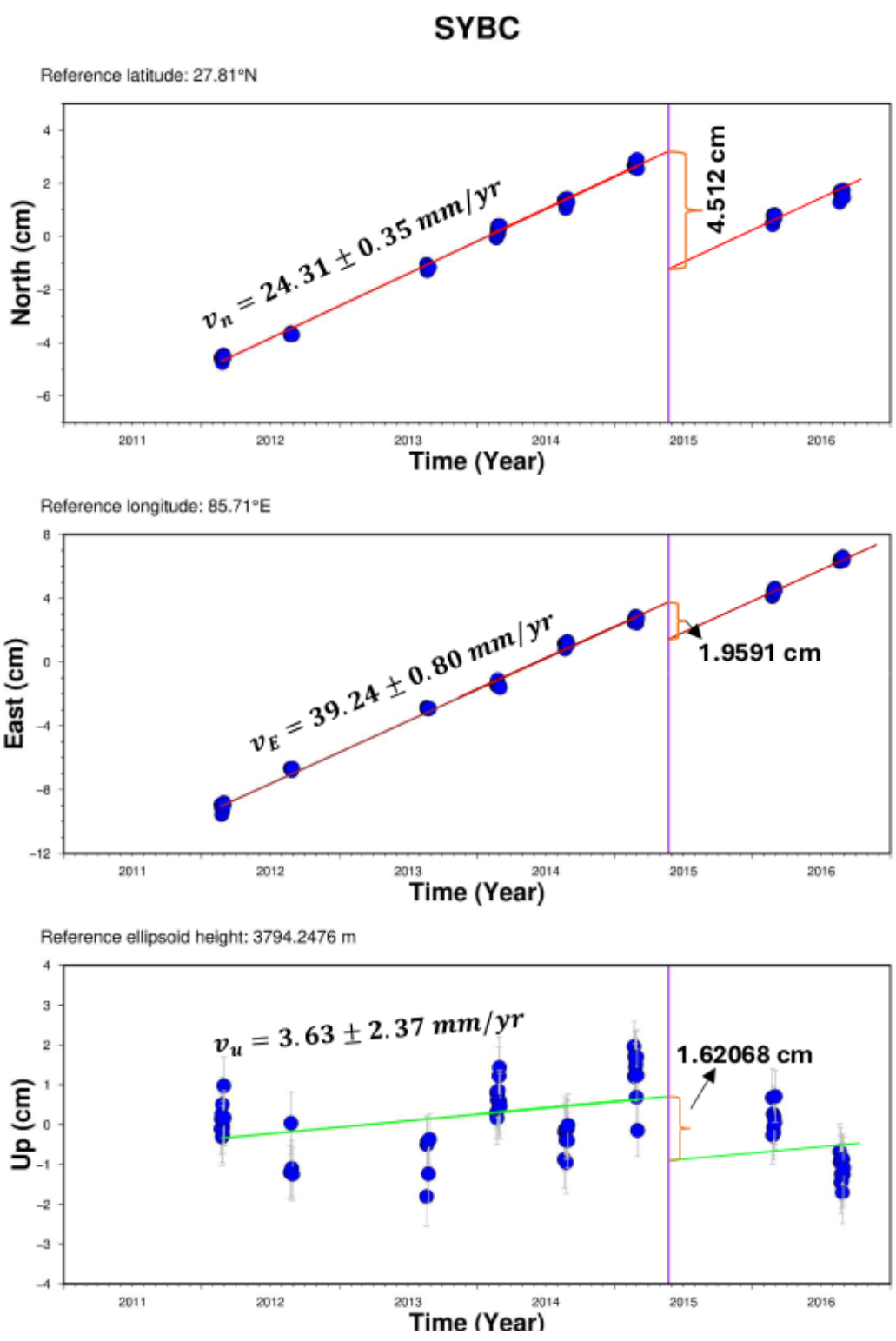

Figure 19. The Velocity of the North component of the station SYBC is 24.31±0.35 mm/yr, the East component is 39.24±0.80 mm/yr, and the vertical component is 3.63±2.37 mm/yr. The crustal deformation of the surface is 4.512 cm, 1.9591 cm, and 1.62068 cm, corresponding to the North, East, and Vertical directions, respectively.

7.2. Outliers

Data points that deviate substantially from the anticipated pattern are called outliers, and they can occur for several reasons, including hardware failures, atmospheric interferences, and human mistakes. Outliers can heavily influence the quality of the results. Therefore, it is crucial to handle them properly to maintain the accuracy and reliability of geodetic outcomes.

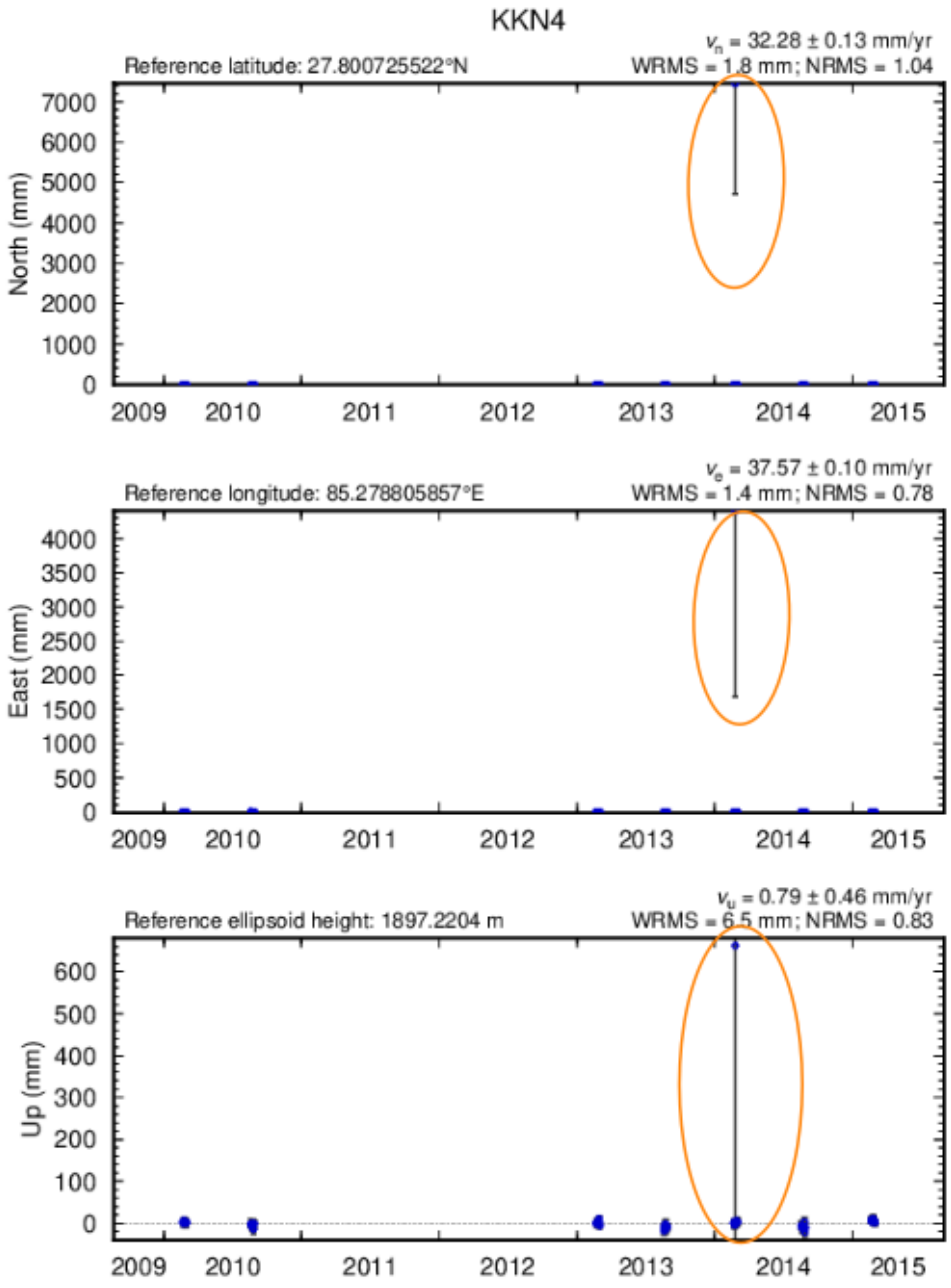

Figure 20. Outliers

7.3. GPS Stations Velocity

The following tables [1] summarize the velocities (in mm/yr) and associated errors for the GPS stations in different directions (North, East and Vertical).

Site	Long	Lat	dEv (mm/yr)	dNv (mm/yr)	E +- (mm/yr)	N +- (mm/yr)	Hvel (mm/yr)	H +- (mm/yr
ARTU	58.56046	56.42982	25.40	6.14	0.34	0.22	-0.11	1.58
BADG	102.23499	51.76970	26.52	-6.47	0.21	0.26	1.77	1.36
BAKO	106.84891	-6.49106	24.54	-7.71	0.43	0.26	0.67	1.30
BESI	84.37967	28.22861	36.95	30.60	0.17	0.30	2.22	1.20
BJFS	115.89249	39.60860	30.35	-10.98	0.39	0.39	1.33	11.16
CHLM	85.31409	28.20723	37.39	26.35	0.47	0.29	4.06	1.25
CHWN	84.38534	27.66824	36.25	31.90	1.16	0.54	2.13	.71
CUSV	100.53392	13.73591	23.76	-9.15	0.33	0.57	-6.75	1.78
DMAU	84.26519	27.97335	37.78	33.27	0.26	0.23	0.57	1.09
DRAG	35.39207	31.59320	23.09	20.28	0.36	0.28	2.05	0.95
GHER	84.40973	28.37460	36.66	27.74	0.10	0.14	5.90	0.46
HARB	27.70725	-25.88696	17.69	18.89	0.47	0.98	2.13	1.75
HYDE	78.55087	17.41726	40.39	35.34	0.47	0.19	1.49	2.33
IISC	77.57038	13.02117	42.13	34.63	0.38	0.33	1.35	1.53
KIRT	85.28816	27.68188	41.46	30.00	0.11	0.14	-29.02	0.47
KKN4	85.27881	27.80073	37.57	32.28	0.18	0.23	0.79	1.10
NAST	85.32773	27.65669	30.39	33.98	1.34	0.65	-112.27	3.12
POL2	4.69427	42.67977	28.09	4.51	0.19	0.16	0.05	0.39
RMJT	86.55001	27.30512	36.88	30.39	0.51	0.15	2.61	2.18
SNDL	85.79886	27.38483	37.79	32.81	0.51	0.41	0.82	1.79
SYBC	86.71246	27.81423	39.24	24.31	0.80	0.35	3.63	2.37
TASH	69.29557	41.32805	25.04	4.20	0.23	0.18	0.85	1.12
TWTF	121.16450	24.95356	34.64	-9.02	0.97	0.67	4.20	0.94

Table 1. Velocity of the different components of the GPS sites

The following figure(21) shows the GPS velocity of the different stations in the Gorkha region of Nepal during the 2015 earthquake.

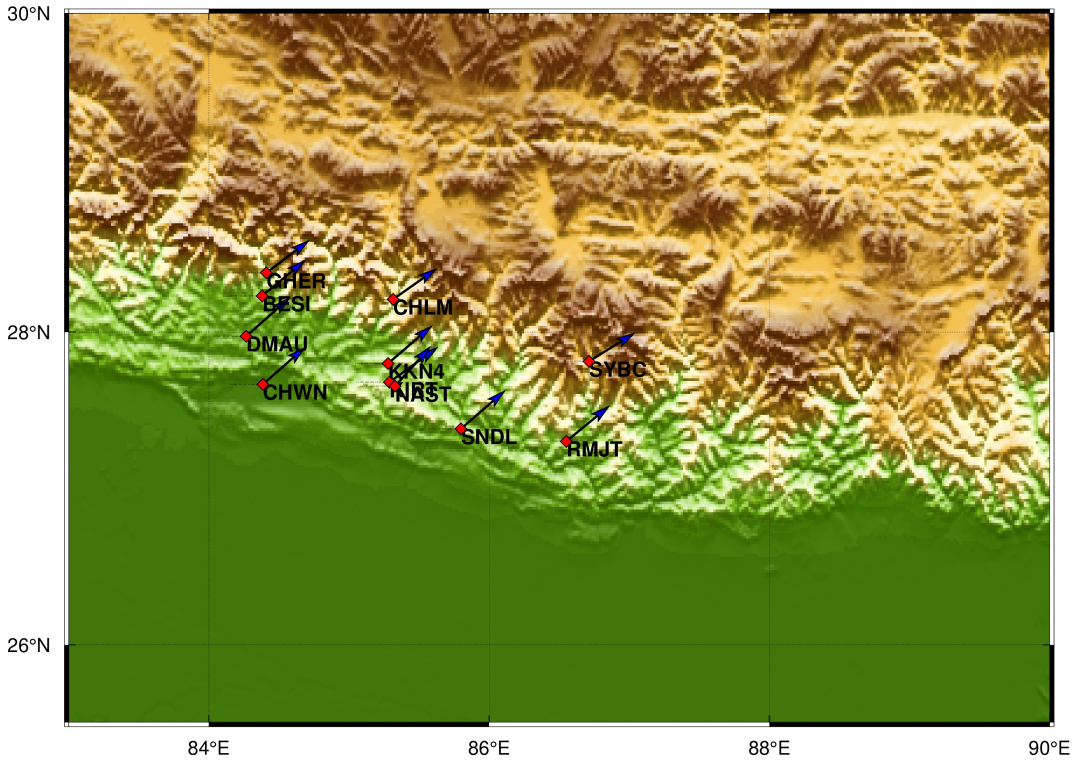

Figure 21. GPS station velocities on the topographic map of Nepal. The arrow indicates the direction of the crustal movement recorded at each station.

8. Conclusions

This study successfully estimated the Crustal deformation in the Gorkha region of Nepal using GPS measurements following the 2015 earthquake. We used GPS data from many stations to study the effects of earthquakes on the Earth's surface. Our analysis revealed significant movement and deformation in the affected areas.

The time series (through GAMIT/GLOBK processing) plot of the different GPS sites in Nepal and IGS stations data and velocity calculations reveal the significant deformation in the region.

The velocities and crustal movements calculated from our GPS measurements indicate varied responses across different stations, reflecting the complex nature of the tectonic interactions in this region.

Stations such as **CHLM, KIRT, KKN4 and NAST** demonstrated significant horizontal and vertical displacements, indicative of the intense tectonic activity triggered by the earthquake.

■ Appendix

This appendix presents the detailed time series plot of the International GNSS Service (IGS) stations used in this study. The plots display the time series data for each station, with the x-axis representing the time (in years) and the y-axis representing the movement of the station in the north, east and vertical directions.

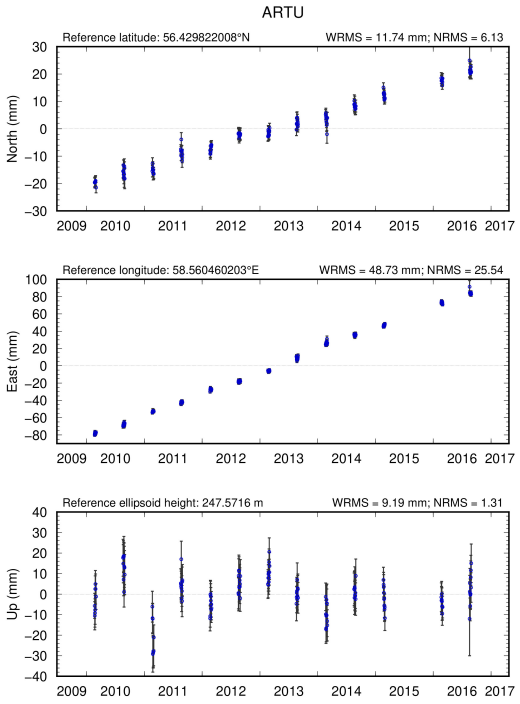

(a) Time series plots for the ARTU GPS station showing displacements in the North (top), East (middle), and Up (bottom) components from 2010 to 2016.

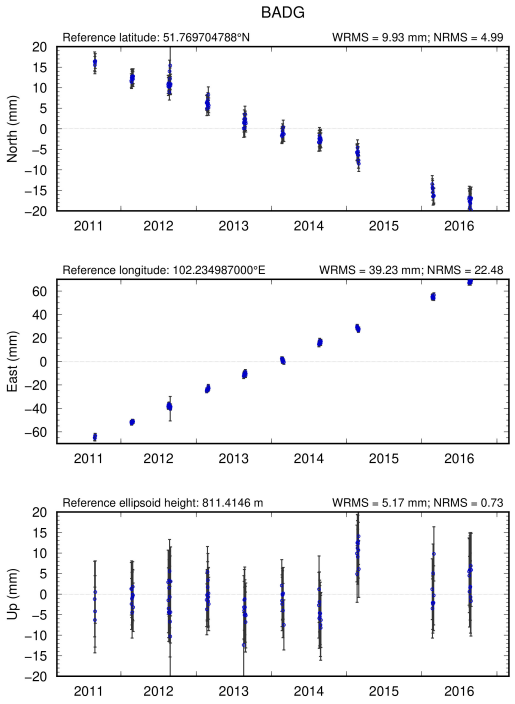

(b) Time series plots for the BADG GPS station showing displacements in the North (top), East (middle), and Up (bottom) components from 2010 to 2016.

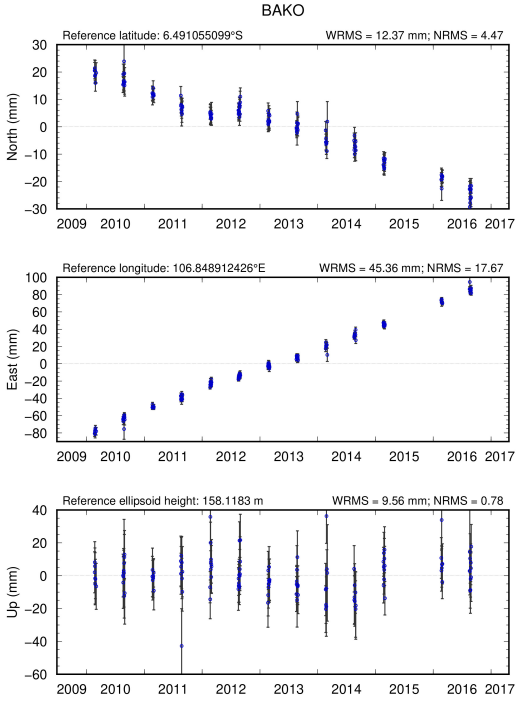

(a) Time-series plot of the station BAKO of North, East and vertical components

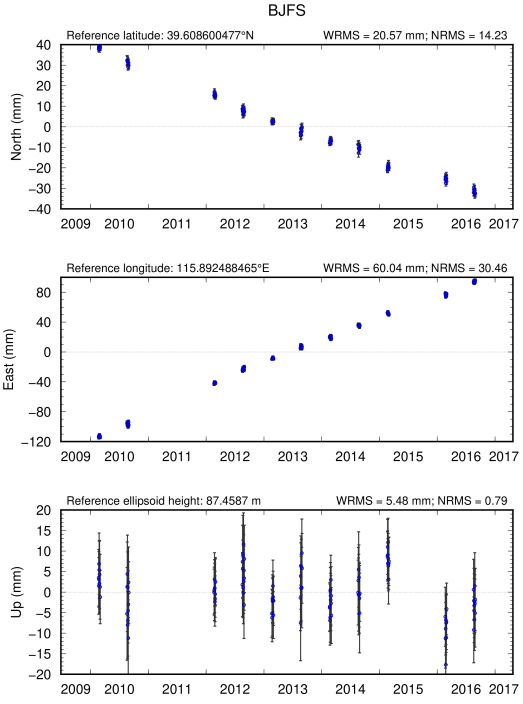

(b) Time-series plot of the station BJFS of North, East and vertical components

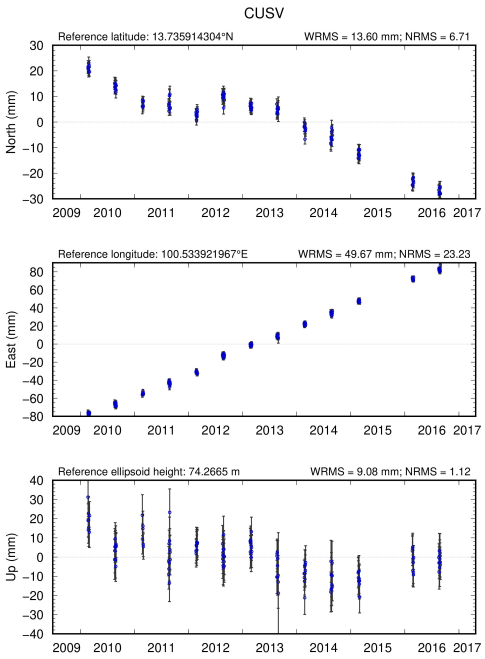

(a) Time-series plot of the station CUSV of North, East and vertical components

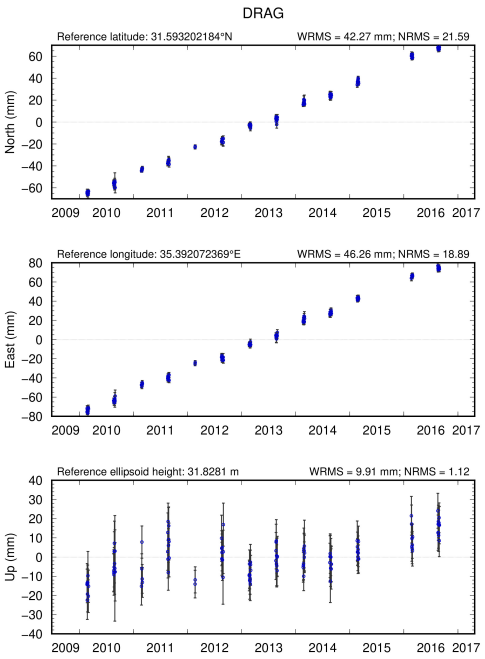

(b) Time-series plot of the station DRAG of North, East and vertical components

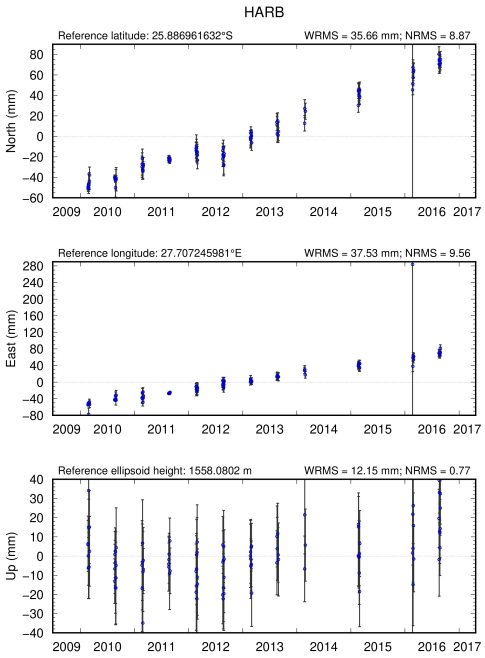

(a) Time-series plot of the station HARB of North, East and vertical components

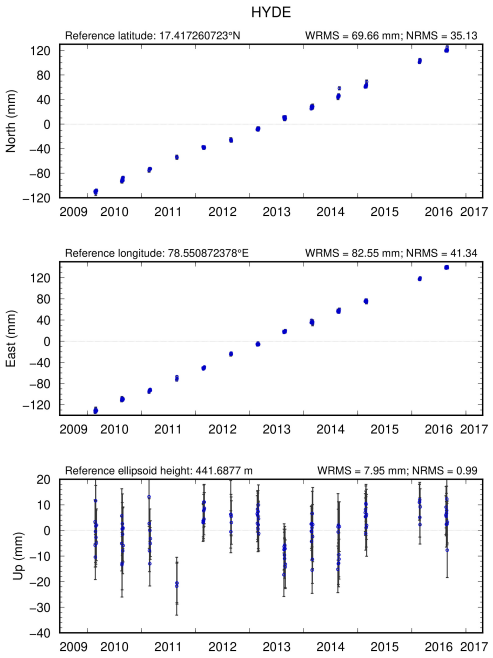

(b) Time-series plot of the station HYDE of North, East and vertical components

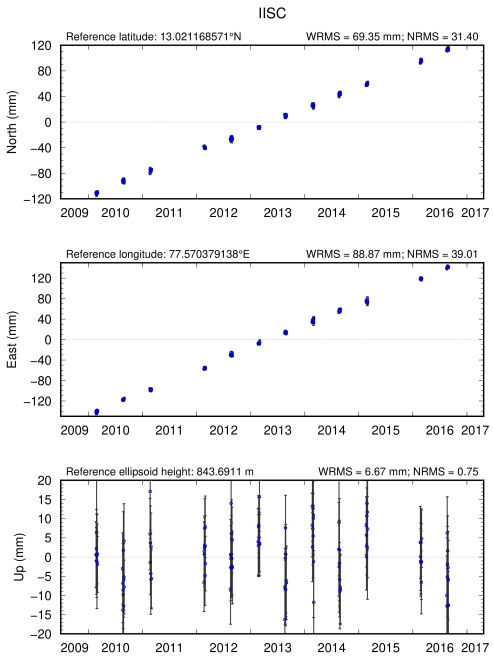

(a) Time-series plot of the station IISc of North, East and vertical components

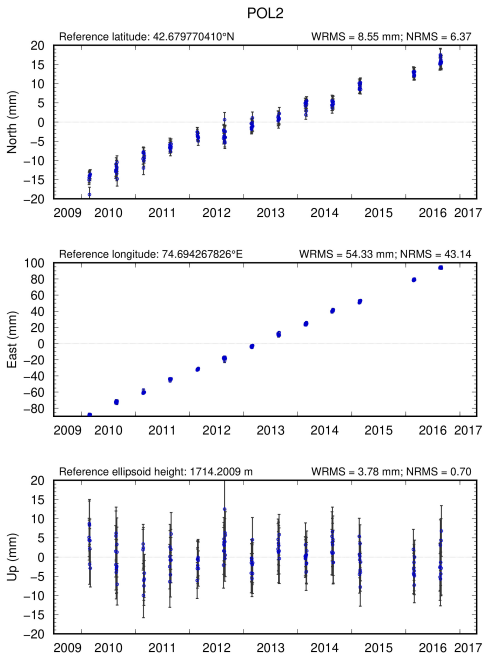

(b) Time-series plot of the station POL2 of North, East and vertical components

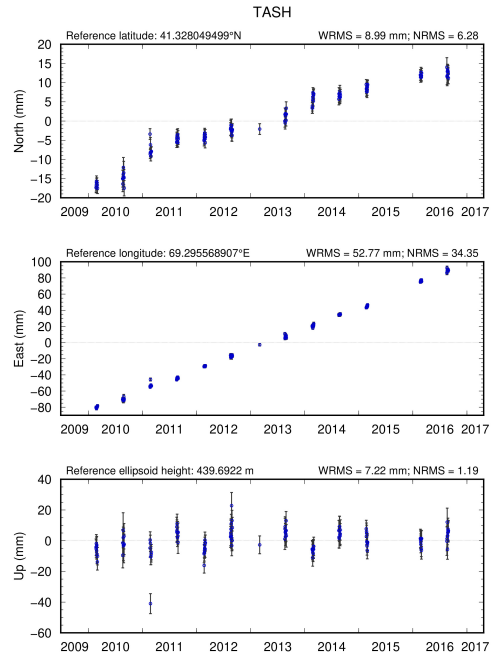

(a) Time-series plot of the station TASH of North, East and vertical components

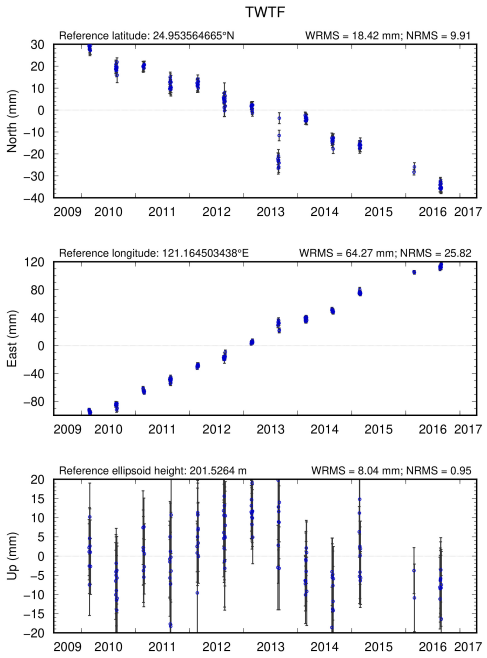

(b) Time-series plot of the station TWTF of North, East and vertical components

References

[1] T. Ader, J.-P. Avouac, J. Liu-Zeng, *et al.*, "Convergence rate across the nepal himalaya and interseismic coupling on the main himalayan thrust: Implications for seismic hazard," *Journal of Geophysical Research: Solid Earth*, vol. 117, no. B4, 2012.

[2] N. Feldl and R. Bilham, "Great himalayan earthquakes and the tibetan plateau," *Nature*, vol. 444, no. 7116, pp. 165–170, 2006.

[3] M. Karaim, M. Elsheikh, A. Noureldin, and R. Rustamov, "Gnss error sources," *Multi-functional operation and application of GPS*, vol. 32, pp. 137–144, 2018.

[4] M. Wang and Z.-K. Shen, "Present-day crustal deformation of continental china derived from gps and its tectonic implications," *Journal of Geophysical Research: Solid Earth*, vol. 125, no. 2, e2019JB018774, 2020.

[5] P. Bettinelli, J.-P. Avouac, M. Flouzat, *et al.*, "Plate motion of india and interseismic strain in the nepal himalaya from gps and doris measurements," *Journal of Geodesy*, vol. 80, pp. 567–589, 2006.

[6] I. Zakharenkova, I. Shagimuratov, N. Y. Tepenitzina, and A. Krankowski, "Anomalous modification of the ionospheric total electron content prior to the 26 september 2005 peru earthquake," *Journal of atmospheric and solar-terrestrial physics*, vol. 70, no. 15, pp. 1919–1928, 2008.

[7] P. Kumar, J. N. Malik, V. K. Gahalaut, R. K. Yadav, and G. Singh, "Evidence of strain accumulation and coupling variation in the himachal region of nw himalaya from short term geodetic measurements," *Tectonics*, vol. 42, no. 8, e2022TC007690, 2023.

[8] T. Herring, "Matlab tools for viewing gps velocities and time series," *GPS solutions*, vol. 7, pp. 194–199, 2003.

[9] Z. Altamimi, P. Rebischung, L. Métivier, and X. Collilieux, "Itrf2014: A new release of the international terrestrial reference frame modeling nonlinear station motions," *Journal of geophysical research: solid earth*, vol. 121, no. 8, pp. 6109–6131, 2016.

[10] S. Schaer, W. Gurtner, and J. Feltens, "Ionex: The ionosphere map exchange format version 1," in *Proceedings of the IGS AC workshop, Darmstadt, Germany*, vol. 9, 1998.

[11] J. Kouba, "Implementation and testing of the gridded vienna mapping function 1 (vmf1)," *Journal of Geodesy*, vol. 82, pp. 193–205, 2008.